



## *In vitro* gastrointestinal stability and Caco-2 cell cytotoxicity of TiO<sub>2</sub> and SiO<sub>2</sub> (nano)particles from confectionary products

Elena Espada-Bernabé, Gustavo Moreno-Martín<sup>\*</sup>, Beatriz Gómez-Gómez, Yolanda Madrid<sup>\*</sup>

Analytical Chemistry Department. Faculty of Chemistry, Complutense University of Madrid, 28040, Madrid, Spain

### ARTICLE INFO

#### Keywords:

spICP-MS  
TiO<sub>2</sub> nanoparticles  
SiO<sub>2</sub> particles  
Confectionary products  
Bioaccessibility  
Caco-2 cells

### ABSTRACT

The effect of an *in vitro* gastrointestinal assay on the characteristics of nanoparticles from food additives TiO<sub>2</sub> (E171) and SiO<sub>2</sub> (E551) present in confectionaries was determined by spICP-MS. No significant differences were detected in particle size distribution regardless of the phase of the *in vitro* stage and the confectionary products, with particles present as aggregates/ agglomerates. The percentage of TiO<sub>2</sub> as nanoparticle form was found to be less than 50 % during the *in vitro* gastrointestinal digestion process, whereas SiO<sub>2</sub> nanoparticles could not be detected due to the high LOD in size obtained (142 nm). The bioaccessible fractions of intestinal extracts showed a 5 % content for both particle types, suggesting their limited absorption in the body. MTT cytotoxicity assay with Caco-2 cells exposed to gastrointestinal extracts from confectionery products revealed an average cytotoxic effect of 40 % for all products tested which was attributed to the food matrix components rather than (nano) particles.

### 1. Introduction

Nanoparticles are gaining increasing significance in food industry, playing diverse roles as additives, flavor enhancers, and components in packaging materials. Ensuring the safety and compliance with regulations of these nanoparticles is of paramount importance to safeguard consumer health (DeLoid et al., 2017; Musial et al., 2020).

Titanium dioxide (TiO<sub>2</sub>), commonly known as food additive E171, and silicon dioxide (SiO<sub>2</sub>) as food additive E551, have become the focus of extensive research due to their ubiquitous presence in various products, ranging from processed foods to nutritional supplements, where they contribute to enhancing physical and aesthetic properties (Geiss et al., 2020; Kesteren et al., 2014). Their analysis is of growing interest owing to their potential impact on food safety and human health (Baranowska-Wójcik et al., 2022). The use of the food additive E171, widely used as whitening agent, has been prohibited by European authorities (The European Commission, 2022), whereas in other regions like the U.S, its utilization remains authorized. Despite the ban on TiO<sub>2</sub> as a food additive, there is still some uncertainty regarding its direct impact on human health. On another note, the food additive E551, commonly used as anticaking agent, maintains its permissibility despite undergoing multiple reassessments by competent authorities (EFSA, 2018). However, it remains under the discerning scrutiny of researchers

by means of conducting toxicity studies on these nanoparticles in humans. The focal point of these studies lies in understanding the fate of these nanoparticles post oral ingestion (Jovanović, 2014). Nevertheless, the available literature lacks *in vitro* assays considering the food matrix in which these nanoparticles are embedded (Cao et al., 2020) and the impact of physicochemical factors occurring along the gastrointestinal tract (variation of pH, presence of carbohydrates, lipids, or proteins) on the characteristics and properties of nanoparticles (DeLoid et al., 2017; McClements et al., 2017; Espada-Bernabé et al., 2024).

Furthermore, the determination of nanoparticles, specifically TiO<sub>2</sub> and SiO<sub>2</sub>, has become critically important due to accumulating evidence suggesting their involvement in instigating inflammatory processes at the cellular level within the intestinal epithelium (Tada-Oikawa et al., 2016; Talamini et al., 2019). This has potential implications for the integrity of the intestinal barrier and the homeostasis of the digestive system. Additionally, recent hypothesis suggests that these nanoparticles might exert an impact on the intestinal microbiota, a key factor affecting gastrointestinal health and the equilibrium of the immune system (Chen et al., 2017; Guilloteau et al., 2022; Yan et al., 2022).

To evaluate the mentioned aspects, the development of analytical techniques is essential to enable a comprehensive characterization of nanoparticles in complex food matrices such as confectionery products (Givélet et al., 2021; Laborda et al., 2016). Among these techniques are

<sup>\*</sup> Corresponding authors.

E-mail addresses: [gusmoren@ucm.es](mailto:gusmoren@ucm.es) (G. Moreno-Martín), [yMadrid@ucm.es](mailto:yMadrid@ucm.es) (Y. Madrid).

electron microscopy techniques, including Transmission Electron Microscopy (TEM) and Scanning Electron Microscopy (SEM) coupled with Energy Dispersive X-Ray (EDX), as well as light scattering techniques like Dynamic Light Scattering (DLS), Nanoparticle Tracking Analysis (NTA), and Multi Angle Light Scattering (MALS) (Brar & Verma, 2011; Verleysen et al., 2019). However, obtaining information on the number and mass concentration with these techniques can be challenging. In last years, spICP-MS (Single Particle Inductively Coupled Plasma Mass Spectrometry) has focused the interest of researchers as it provides relevant information on nanoparticles physicochemical properties (size distribution, number and mass concentration or ionic concentration) (Laborda et al., 2014; Mozhayeva & Engelhard, 2020).

Therefore, the main goal of the current study focuses on investigating the gastrointestinal fate of TiO<sub>2</sub> and SiO<sub>2</sub> (nano)particles found in samples of confectionery products (pure cocoa, soluble cocoa, and powdered custard) by using an *in vitro* gastrointestinal assay and the Caco-2 cell line. The morphology, aggregation/agglomeration state, size distribution and particle number concentration at each stage of the process will be determined by TEM and spICP-MS techniques and percentage of bioaccessibility will be calculated. Moreover, Caco-2 cell line will be exposed to the intestinal fractions, and cell viability will be assessed at various exposure times using the MTT colorimetric assay.

## 2. Materials and methods

### 2.1. Samples

In this study, the confectionery products (pure cocoa powder, soluble cocoa powder, and powdered custard) that may contain TiO<sub>2</sub> and/or SiO<sub>2</sub> (nano)particles were subjected to an *in vitro* gastrointestinal digestion model. All these products were acquired from supermarkets in the Community of Madrid, Spain.

Ingredient lists of each confectionery product can be found in [Supplementary material](#).

### 2.2. Titanium and silicon total content

Total titanium and silicon content in the confectionery products was performed by an Agilent 7700x ICP-MS (Agilent Technologies Inc., USA) instrument, after acid digestion in a microwave oven (MSP 1000, CEM, Matheus, NC). The mineralization protocol was adjusted based on Espada-Bernabé et al., 2024, with a modification to set the sample mass at 100 mg. For both titanium and silicon quantification, an external calibration was established using a dissolved titanium and silicon ionic standard (Merck, Spain) ranging from 0 to 100 µg L<sup>-1</sup> and 0 to 500 µg L<sup>-1</sup>, respectively with an acid content equivalent to that of samples resulting from the digestion procedure. Data was collected under continuous acquisition mode by monitoring <sup>48</sup>Ti and <sup>28</sup>Si isotopes. Detection and quantification limits were calculated as three and ten times the blank standard deviation, respectively (IUPAC, 1978). The experimental parameters were set as follows: RF power at 1550 W, sample depth of 8 mm, plasma gas flow rate of 15.0 L min<sup>-1</sup>, auxiliary gas flow rate of 0.90 L min<sup>-1</sup>, and a Micromist nebulizer with a flow rate of 1.01 L min<sup>-1</sup>. Daily adjustments of ICP-MS parameters, including nebulization gas flow, torch position, optical lenses, and quadrupole voltages, were carried out. Analyses were performed in triplicate.

### 2.3. *In vitro* gastrointestinal digestion assay. Study of bioaccessibility of TiO<sub>2</sub> and SiO<sub>2</sub> (nano)particles from confectionery products

An *in vitro* gastrointestinal digestion process implies the application of different centrifugation steps along the process. In a previous study, Espada-Bernabé et al.(2024) showed that centrifugation (speed and time) has a notably effect on TiO<sub>2</sub> particles sedimentation, being the 1500 rpm and 5 min the optimal conditions. Therefore, same centrifugation conditions (5 and 10 min at 1500, 4000, 6000, and 10000 rpm

speeds) were evaluated for SiO<sub>2</sub> (200 nm Silica Nanospheres. Nano-composix, Spain) aqueous particle standard by spICP-MS measurements.

The *in vitro* simulated gastrointestinal digestion experiments were carried out under the same conditions described by Espada-Bernabé et al.(2024), consisting of three distinct phases (namely salivary, gastric and intestinal). Briefly, 1.0000 g of each confectionery product was dissolved in 10 mL of Milli-Q water. In the salivary step, the 10 mL of aqueous extract was combined with 5 mL of *in vitro* synthesized saliva containing α-amylase, agitating the mixture at 200 rpm and maintained at 37 °C for 15 min. Subsequently, 12 mL of gastric solution containing pepsin were added and the solutions were acidified to a pH of 1.8 using HCl and maintained under stirring at 200 rpm at 37 °C for 2 h. The gastric process was stopped by raising the pH to 6.8 using a saturated sodium bicarbonate solution. Finally, 17 mL of simulated intestinal fluid that includes pancreatin were added to simulate the intestinal phase, and the resulting solutions were subsequently incubated at 200 rpm and 37 °C for 2 h. Aliquots of each step were taken for its further characterization by TEM and spICP-MS as changes in (nano)particle size, morphology and aggregation state may occur and by ICP-MS to assess the total content of titanium and silicon in each *in vitro* gastrointestinal stage. The acid digestion mixture and conditions were applied as described in [section 2.2](#). Three replicates were performed for each confectionery product.

Moreover, the bioaccessibility percentage was also calculated from each gastrointestinal stage using Eq. (1):

$$\%Bioaccessibility = \frac{[Ti/Si]_{totalgastrointestinalextract}}{[Ti/Si]_{totalcontent}} \times 100 \quad (1)$$

where [Ti/Si]<sub>total gastrointestinal extract</sub> refers to the total titanium or silicon content identified in the salivary, gastric, or intestinal extracts, while [Ti/Si]<sub>total content</sub> represents the total titanium or silicon content found in the food products after acid digestion process described in [Section 2.2](#). This formula provides an estimate of the proportion of Ti/Si that is bioaccessible or available for being absorbed after the gastrointestinal digestion process.

### 2.4. Assessment of changes in the physicochemical properties of TiO<sub>2</sub> and SiO<sub>2</sub> (nano)particles during the *in vitro* gastrointestinal digestion process

Since the conditions of the different stages of *in vitro* gastrointestinal digestion assay can affect several physicochemical properties of the particles studied, such as size, aggregation/agglomeration state, and morphology; complementary techniques have been employed to assess the change in these properties.

Hence, it is essential to compare the different particle parameters before and after the gastrointestinal digestion process. To determine the physical-chemical characteristics of nanoparticles before performing the *in vitro* gastrointestinal assay, confectionery products were treated with water following the adapted procedure described by Espada-Bernabé et al.(2024). In summary, 100 mg of the sample was suspended in 10.0 mL of Milli-Q water and manually shaken for 10 min to quantitatively extract the (nano)particles. On the other hand, the fractions of the gastrointestinal extracts were obtained as described in [Section 2.3](#).

#### 2.4.1. TEM analysis

The collected fractions from each stage of the *in vitro* gastrointestinal digestion study were characterized in terms of morphology and aggregation/agglomeration state by TEM. Around 25 µL aliquots from each stage of the gastrointestinal process were collected and placed onto copper grids and allowed to air-dry. These dried samples were then subjected to TEM and energy dispersive X-ray spectroscopy (EDX) measurements with a JEOL JEM 1400 PLUS instrument, which operates at 140 kV and is equipped with a CCD camera (KeenView Camera) (JEOL Ltd., Tokyo, Japan). Constituent particle size and distributions from TEM micrographs were obtained according to rule number 4 of Part 3:

Standard operating Procedures (SOPs) from The NanoDefine Methods Manual (Mech et al., 2020).

#### 2.4.2. spICP-MS analysis

TiO<sub>2</sub> and SiO<sub>2</sub> (nano)particles size distribution and concentration (part L<sup>-1</sup> or part g<sup>-1</sup>) derived from each *in vitro* gastrointestinal digestion stage were assessed by spICP-MS. An Agilent 7700x quadrupole ICP-MS was employed, featuring a peristaltic pump, a Micromist nebulizer, a cooled Scott-type spray chamber, and a standard quartz torch with a 1.0 mm inner diameter. A dwell time of 3 ms was established, and the overall data acquisition time was set to 60 s. Operational parameters were set daily to achieve peak sensitivity. The transport efficiency was calculated using a diluted 30 nm quality control material of citrate-coated gold nanoparticles (AuNPs) (LGCQC5050) at a concentration of 20 ng L<sup>-1</sup> and monitoring <sup>197</sup>Au signal. Transport efficiency mean value of 3.7 ± 0.2 % was calculated according to the particle frequency method developed by Pace et al. (2011). A mean flow rate of 0.30 ± 0.02 mL min<sup>-1</sup> was daily gravimetrically calculated as the variation in mass of Milli-Q water introduced into the equipment over a period of 15 min.

To mitigate the interference of particle signals-background overlap, and double events in spICP-MS measurements, substantial dilution factors were employed for the samples, as outlined by Bolea-Fernández et al. (2017). The diluted sample suspensions produced around 600–1200 particles detected during the selected acquisition time. This particle number considers particle concentration ranges between 2·10<sup>6</sup> to 2·10<sup>8</sup> particles L<sup>-1</sup>, deemed enough to ensure a statistically sound particle size distribution under these experimental conditions according to standard operating procedure proposed by Mech et al. (2020) in The NanoDefine Methods Manual Part 3: Standard operating Procedures (SOPs). In addition, for each stage, data were acquired in triplicate for the <sup>48</sup>Ti and <sup>28</sup>Si isotopes separately. Calibration curve of ionic Ti and Si ranging from 0 to 75 µg L<sup>-1</sup> and 0 to 500 µg L<sup>-1</sup>, respectively, were prepared daily by employing ionic standard solutions for ICP-MS.

Raw signal intensity data were processed using the free RIKILT spreadsheet for Microsoft Excel described by Peters et al. (2015). This facilitated the calculation of particle number concentration and particle mass concentration. For obtaining TiO<sub>2</sub> particle size a TiO<sub>2</sub>/Ti ratio of 1.667 and a density of 3.9 g cm<sup>-3</sup> (anatase phase) were selected. This choice is based on anatase being the predominant crystalline form employed for producing food-grade TiO<sub>2</sub> (EFSA Panel on Food Additives and Flavourings (FAF), 2019). TiO<sub>2</sub> (nano)particles measurements by spICP-MS were validated with a TiO<sub>2</sub> powder referred as NM-100-JRCNM10200 from the European Commission Joint Research Center (JRC) (Ispra, Italy) being composed mainly of anatase. According to a characterization carried out by JRC using TEM, the TiO<sub>2</sub> particles of NM-100 have a mean diameter of 190.6 ± 5.8 nm (European Commission. JRC, 2014). For SiO<sub>2</sub> particles, a SiO<sub>2</sub>/Si ratio of 2.143 and a density of 2.6 g cm<sup>-3</sup> were set to obtain the same parameters as above. SiO<sub>2</sub> determinations by spICP-MS were validated with 200 nm Silica NanoSpheres (Nanocomposix, California). For the characterization of both (nano)particles in terms of size (diameter) and concentrations it was assumed that the particles are spherical.

#### 2.5. Effect of intestinal extracts on Caco-2 cells viability by MTT assay

MTT assay allows to evaluate the cytotoxicity of intestinal extracts containing TiO<sub>2</sub> and SiO<sub>2</sub> (nano)particles on Caco-2 cells.

Human Caco-2 cells (ATCC, American Type Culture Collection, U.S.) were cultured in DMEM (Dulbecco's Modified Eagle Medium) (Fisher Scientific, Spain) supplemented with 10 % FBS (Fetal Bovine Serum) and 5 % penicillin–streptomycin. The cells were incubated and maintained in plastic dishes at 37 °C in a humidified atmosphere of 5 % CO<sub>2</sub>. Culture medium was refreshed every 2 to 3 days until the cells reached 80 % confluence. Upon this point, the cells were dissociated using PBS (Phosphate-Buffered Saline) (Fisher Scientific, Spain) at pH 7.4 and Trypsin-EDTA (0.05 %) (Fisher Scientific, Spain). Cells were

resuspended in DMEM.

To evaluate the potential effect of ionic titanium and silicon, TiO<sub>2</sub> and SiO<sub>2</sub> as (nano)particles and its overall effect on cell viability, Caco-2 cells were exposed to the different chemical forms at concentration found in intestinal extracts after *in vitro* digestion. Consequently, concentrations of 20 and 40 µg L<sup>-1</sup> for ionic titanium (Merck, Spain), 200 and 1000 µg L<sup>-1</sup> for ionic silicon (Merck, Spain), 1 and 10 µg L<sup>-1</sup> (10<sup>6</sup>–10<sup>7</sup> part g<sup>-1</sup>) for particulate TiO<sub>2</sub> (Merck, Spain) and SiO<sub>2</sub> (10<sup>6</sup>–10<sup>7</sup> part g<sup>-1</sup>) (200 nm Silica NanoSpheres. NanoComposix, California) were evaluated on cell viability of Caco-2 cells by MTT assay. For that purpose, 15,000 cells per plate (optimized number) were seeded in a 96-well plate and maintained with DMEM at 37 °C in a humidified atmosphere of 5 % CO<sub>2</sub> overnight. Negative controls with only culture medium in absence of cells and positive controls, containing cells in DMEM supplemented with 10 % FBS, were also evaluated. The culture medium was then removed, and the cells were exposed to the commercial solutions, during 4 and 24 h. In the case of positive and negative controls, an equivalent volume of culture medium was added instead of FBS. After each incubation time, the culture media was removed, 20 µL of a 5 mg mL<sup>-1</sup> MTT solution was added, and cells were then incubated under identical conditions for 4 h. Afterwards, the MTT solution was removed, and the resulting formazan crystals were dissolved in 100 µL of DMSO. Finally, the absorbance was measured at 570 nm using a microplate reader (Fisher Scientific, Hampton, EEUU).

The same protocol was applied on Caco-2 cells exposed to intestinal extracts and their respective blanks (intestinal solution) after *in vitro* digestion, both diluted by a factor of 1/10 in DMEM supplemented with 10 % FBS. The same dilution factor was applied to ionic titanium and silicon and to TiO<sub>2</sub> and SiO<sub>2</sub> as (nano)particle standards.

#### 2.6. Statistical analysis

One- and two-way ANOVA analysis were performed to identify any statistically significant differences during the gastrointestinal process concerning the concentration and constituent particle size of each analyzed confectionery product. The ANOVA analysis was conducted using Statgraphics 18 software.

### 3. Results and discussion

#### 3.1. Total content of titanium and silicon in confectionary products

The ICP-MS analysis was employed to determine the total silicon and titanium content in the confectionery products chosen for this study. This was conducted after subjecting the samples to an acid mineralization process, aiming to uncover the potential presence of TiO<sub>2</sub> and SiO<sub>2</sub> as these compounds might not always be explicitly listed as food ingredients.

Interferences for most abundant isotopes of both elements, <sup>48</sup>Ti (73.73 % of relative isotopic abundance) and <sup>28</sup>Si (92.23 %), were carefully considered. In the case of <sup>48</sup>Ti, the potential polyatomic interferences from <sup>32</sup>S<sup>16</sup>O and <sup>36</sup>Ar<sup>12</sup>C, and the isobaric interference of <sup>48</sup>Ca are well reported in literature (Bucher & Auger, 2019; Peters et al., 2014). For this reason, <sup>48</sup>Ca (0.187 %) was also monitored in both the samples and the blanks, with no significant differences found in the signals. It was therefore concluded that the calcium signal was low enough to have no effect on titanium.

Regarding <sup>28</sup>Si isotope, there are numerous works in the literature referring to the significant polyatomic interferences, such as <sup>12</sup>C<sup>16</sup>O and <sup>14</sup>N<sub>2</sub><sup>+</sup>, of this isotope when measured in a single quadrupole ICP-MS (Bolea-Fernández et al., 2017). Trying to minimize these interferences, both <sup>28</sup>Si and <sup>29</sup>Si isotopes were monitored with and without H<sub>2</sub> as gas cell. No significant improvements in sensitivity were observed, resulting for <sup>28</sup>Si LODs of 40 and 39 µg L<sup>-1</sup> for non-gas and gas mode, respectively. Hence, <sup>28</sup>Si isotope was monitored for subsequent measurements in non-gas mode.

There were no significant differences in LOD and LOQ values for titanium between Milli-Q water and confectionery product extracts, with a LOD of  $5 \mu\text{g L}^{-1}$  and a LOQ of  $14 \mu\text{g L}^{-1}$ . However, silicon showed variations, with Milli-Q water providing a LOD of  $40 \mu\text{g L}^{-1}$  and a LOQ of  $121 \mu\text{g L}^{-1}$ , while confectionery products displayed higher values, with LODs ranging from  $74$  to  $86 \mu\text{g L}^{-1}$  and LOQs from  $223$  to  $262 \mu\text{g L}^{-1}$ .

Matrix effect was also evaluated, as confectionery products are complex samples. The comparison of slopes between standard addition and external calibration revealed no significant differences ( $p > 0.05$ ) for any of the confectionery products.

Both titanium and silicon were also quantified in all examined confectionery products as indicated in Table 1. Comparable levels of titanium were measured in pure cocoa powder, soluble cocoa powder, and powdered custard. By contrast, silicon contents varied significantly among the different products, generally displaying higher concentrations compared to titanium, as expected according to its high abundance in Earth's crust (Silicon is the second most abundant element after oxygen).

### 3.2. Bioaccessibility of $\text{TiO}_2$ and $\text{SiO}_2$ (nano)particles from confectionery products

To assess the availability of  $\text{TiO}_2$  and  $\text{SiO}_2$  (nano)particles for absorption in the intestine, the bioaccessibility percentages were calculated for the different confectionery products. The total Ti/Si content was measured in each stage of the gastrointestinal process (Section 2.3), as well as the total content of the products before gastrointestinal simulation (Section 2.2).

According to the data collected in Table 2 the highest bioaccessibility values was obtained for silicon in soluble cocoa, with silicon presenting a higher bioaccessibility than titanium regardless the confectionery product in the *in vitro* intestinal stage.

### 3.3. Variations in particle concentration, size distribution, constituent particle size, and morphology throughout the gastrointestinal tract

Particles contained in confectionery products can undergo changes in their physicochemical properties along the gastrointestinal tract. These changes can be related to morphology, particle concentration, and size distribution as (nano)particles interact with different biological components employed in the *in vitro* digestion assay. In addition, pH variations at each stage of the gastrointestinal process could play an important role in these changes.

Quantitative information such as size distribution and particle concentration could not be obtained from TEM analysis. In the micrographs shown in Fig. 1 for all confectioneries extracts, aggregated particles of small size were observed. Due to the complexity of the extracts in terms of food matrix, enzymatic composition as well as the low levels of  $\text{TiO}_2$  and  $\text{SiO}_2$  particles, it was not possible to obtain a significant number of particles to determine particle size. The presence of  $\text{SiO}_2$  particles was confirmed by EDX ( $K\alpha$  (1.740 keV)) for all the confectionery products. However, titanium signal was only detected for powdered custard ( $K\alpha$  (4.508 keV) and  $L\alpha$  (0.452 keV)) in salivary stage, which could be attributed to the low level of Ti found in the extracts.

Since no quantitative information could be obtained by TEM, spICP-MS analysis was performed under the conditions previously described in

**Table 1**

Total titanium (Ti) and silicon (Si) content in pure and soluble cocoa, and custard powder assessed by ICP-MS.

Food matrix	$^{28}\text{Si} \mu\text{g g}^{-1}$	$^{48}\text{Ti} \mu\text{g g}^{-1}$
Pure cocoa	$2172 \pm 50$	$50 \pm 1$
Soluble cocoa	$1315 \pm 27$	$34 \pm 1$
Powdered custard	$387 \pm 40$	$38 \pm 1$

Results expressed as the mean value  $\pm$  SD for  $n = 3$  determination.

**Table 2**

Titanium (Ti) and silicon (Si) percentages from salivary, gastric and intestinal stages. Data obtained by ICP-MS.

<i>In vitro</i> digestion stage	% Titanium			% Silicon		
	Pure cocoa	Powdered custard	Soluble cocoa	Pure cocoa	Powdered custard	Soluble cocoa
Salivary	$8 \pm 1$	$10 \pm 1$	$9 \pm 2$	$20 \pm 4$	$5 \pm 2$	$3 \pm 1$
Gastric	$9 \pm 1$	$11 \pm 2$	$40 \pm 7$	$40 \pm 8$	$2 \pm 1$	$3 \pm 1$
Intestinal	$19 \pm 3$	$18 \pm 1$	$45 \pm 10$	$45 \pm 9$	$26 \pm 5$	$78 \pm 2$

Results expressed as the mean value  $\pm$  SD for  $n = 3$  determination.

section 2.4.2. The  $5\sigma$  criterion ( $\sigma$ : standard deviation from baseline) was applied to distinguish between background signals and particulate matter, thus mitigating the occurrence of false positives in the spICP-MS analysis (Laborda, Giménez-Inglaturre, Bolea, & Castillo, 2020). This approach considers the frequency distribution of recorded events, represented via histograms. Applying this criterion,  $\text{LOD}_{\text{size}}$  of 30 nm for  $\text{TiO}_2$  and 142 nm for  $\text{SiO}_2$  in Milli-Q water were obtained. The high  $\text{LOD}_{\text{size}}$  value for  $\text{SiO}_2$ , observed when measurements were conducted using a single quadrupole ICP-MS, hindered the detection and quantification of nanoparticulate material below 100 nm.

As for conventional ICP-MS determinations (Section 3.1), the interferences of each isotope analyzed were considered in the spICP-MS measurements. For  $\text{TiO}_2$  determinations in non-gas mode, isobaric interference between  $^{48}\text{Ti}$  and  $^{48}\text{Ca}$  was addressed by monitoring  $^{48}\text{Ca}$  in the samples. Low levels of calcium were detected as a continuous background, from which  $^{48}\text{Ti}$  could be clearly differentiated. Therefore, the  $^{48}\text{Ti}$  isotope was monitored in non-gas mode. Similar conclusions were reported by Bucher & Auger (2019) when analyzing food products containing E171, suggesting that the mentioned isobaric interference can be disregarded when measuring this isotope in such samples using spICP-MS.

For silicon, the high backgrounds posed a challenge in distinguishing the particles from the ionic background. Similar to conventional ICP-MS determinations,  $\text{H}_2$  was tested as a collision gas to achieve a signal background between  $0\text{--}5 \mu\text{g L}^{-1}$  (Bolea-Fernández et al., 2017), but no significant improvements in the recorded backgrounds were found.

Due to the lack of  $\text{TiO}_2$  reference material, the results were validated by the analysis of NM-100-JRCNM10200, which was extensively characterized in terms of size (European Commission. JRC, 2014). According to JRC, the average diameter of  $\text{TiO}_2$  particles in the NM-100-JRCNM10200 material is  $190.6 \pm 5.8$  nm, with a nanoparticulate fraction of 27.1 %. Comparable results, with a constituent particle size of  $193 \pm 5$  nm and a nanoparticulate fraction of  $25 \pm 2$  %, were obtained when measuring this material under the conditions described in section 2.4.2. In addition, the obtained results for this material were comparable to those obtained by Bastardo-Fernández et al. (2023), who performed the measurements by using a spICP-MS/MS with a high efficiency sample introduction system. On the other hand, the validation of the  $\text{SiO}_2$  results obtained by spICP-MS, in terms of size, was performed using a 200 nm standard Silica Nanospheres. The constituent particle size obtained by monitoring  $^{28}\text{Si}$  was  $200 \pm 6$  nm.

A key factor in evaluating changes in the physicochemical properties of nanoparticles and obtaining consistent results is to avoid nanoparticle sedimentation during the centrifugation steps applying between gastrointestinal digestion phases. Therefore, preliminary centrifugation tests were performed at the specified times and speeds outlined in Section 2.3. The selected optimal centrifugation conditions for both particles were 5 min at a speed of 1500 rpm, resulting in recoveries of  $89 \pm 6$  % for  $\text{TiO}_2$  and  $93 \pm 2$  % for  $\text{SiO}_2$ , obtained by spICP-MS analysis. Once selected the optimal centrifugation conditions, samples were submitted to the *in vitro* gastrointestinal digestion process and the resulting extracts obtained after applying the optimized centrifugation conditions from

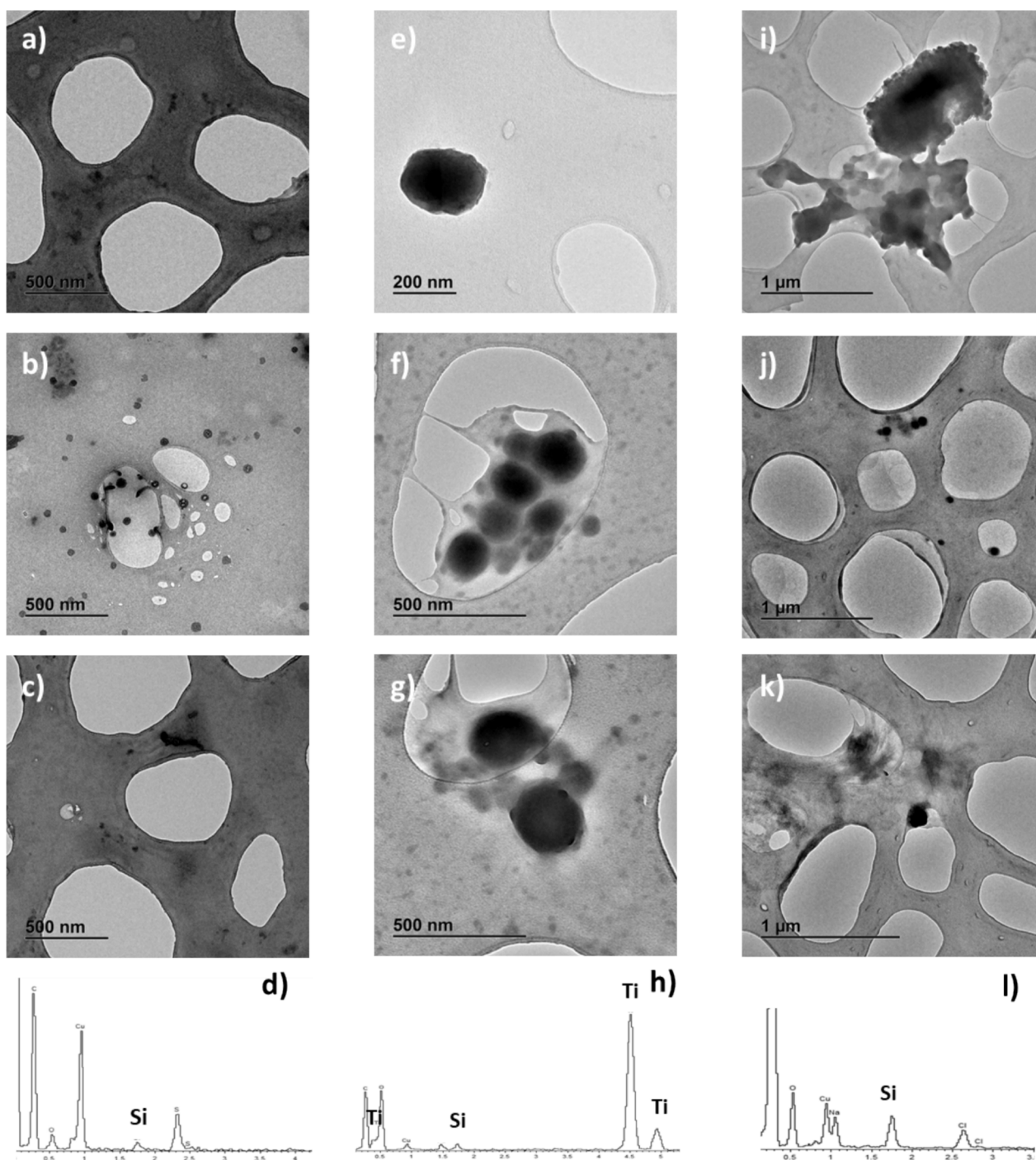


**Fig. 1.** TEM micrographs of soluble cocoa (a), b) and c)), powdered custard (e), f) and g)), pure cocoa (i), j) and k)) extracts across gastrointestinal simulation stages a), e) and i) salivary, b), f) and j) gastric and c), g) and k) intestinal. Figures d), h) and l) shows EDXs signals from each simulation stage, respectively.

each step were measured by spICP-MS (Section 2.4.2). The analysis of the extracts from the different gastro-intestinal steps allowed us to determine the step with the major incidence on the size and concentration of nanoparticles. It is important to emphasize that the use of enzymes resulted in an increase in the signal background for both elements. The  $LOD_{size}$  for  $TiO_2$  increased from 30 to 63, 56, and 61 nm in the salivary, gastric, and intestinal phases, respectively. However, for  $SiO_2$ , a significant increase in the signal background was only observed in the intestinal stage, resulting in an increase in the  $LOD_{size}$  from 142 nm in water, salivary, and gastric phases to 151 nm in the intestinal phase. In addition, it is important to highlight that no  $TiO_2$  or  $SiO_2$  particles were detected in the salivary, gastric or intestinal enzymatic

blanks.

The size variations of  $TiO_2$  and  $SiO_2$  (nano)particles detected in saliva, gastric, and intestinal extracts for each confectionary product studied are shown in Table 3. No significant differences ( $p > 0.05$ ) were found in the constituent particle size and size distribution of  $TiO_2$  particles between different phases of the *in vitro* gastrointestinal digestion of the confectionary products when performing one-way ANOVA analysis. Our results partially agreed with those reported by Ferraris et al.(2023) and Bettencourt et al.(2020) where size distribution of particles derived from bulk food additive E171 remains unaltered during *in vitro* simulation.

Similarly, the size distribution of  $SiO_2$  particles remains unaltered (p

**Table 3**

TiO<sub>2</sub> and SiO<sub>2</sub> (nano)particle characterization in terms of mean size, percentages under 100, 250 and 500 nm before and after the *in vitro* gastrointestinal digestion steps for pure cocoa, custard powder and soluble cocoa. Measurements were performed by spICP-MS.

		TiO <sub>2</sub> particles			SiO <sub>2</sub> particles		
		Constituent particle size (nm)	<100 nm (%)	<250 nm (%)	Constituent particle size (nm)	<250 nm (%)	<500 nm (%)
Pure cocoa	Water	126 ± 40	30 ± 4	98 ± 3	269 ± 27	32 ± 7*	100
	Salivary	127 ± 37	24 ± 6	98 ± 5	257 ± 61	67 ± 12	100
	Gastric	128 ± 39	25 ± 4	98 ± 5	248 ± 65	64 ± 11	99 ± 2
	Intestinal	134 ± 28	ND	99 ± 6	238 ± 60	69 ± 11	99 ± 3
Powdered custard	Water	147 ± 72	36 ± 7	97 ± 2	278 ± 36	37 ± 9*	98 ± 5
	Salivary	145 ± 41	38 ± 5	98 ± 2	258 ± 60	85 ± 13	99 ± 3
	Gastric	146 ± 34	37 ± 6	97 ± 5	220 ± 47	80 ± 11	99 ± 3
	Intestinal	151 ± 42	ND	97 ± 4	261 ± 54	86 ± 9	98 ± 4
Soluble cocoa	Water	125 ± 65	48 ± 6	97 ± 4	271 ± 21	43 ± 11*	100
	Salivary	156 ± 28	ND	99 ± 3	218 ± 36	82 ± 15	100
	Gastric	149 ± 27	ND	97 ± 5	207 ± 39	87 ± 17	100
	Intestinal	167 ± 40	ND	93 ± 4	235 ± 28	83 ± 10	100

ND: not detected.

\* Indicates statistically significant differences ( $p < 0.05$ ) within the same column before (water) and under *in vitro* conditions (salivary, gastric and intestinal).

> 0.05) during the different phases of *in vitro* gastrointestinal digestion process according to one-way ANOVA. In other reported studies the results obtained are contradictories, Peters et al.(2012), indicated the formation of SiO<sub>2</sub> agglomerates during gastric digestion whereas McClements et al.(2016) showed that an increase in pH during the gastric phase could induce the deagglomeration of SiO<sub>2</sub> particles. In our case, only SiO<sub>2</sub> particles larger than 142 nm were detectable and quantifiable because of the LOD<sub>size</sub> values according to the single quadrupole ICP-MS used in the measurements. As it can be seen in Table 3, in the case of TiO<sub>2</sub>, the percentage of TiO<sub>2</sub> as nanoparticle form is less than 50 % during the different phases of the *in vitro* gastrointestinal digestion process. In the case of SiO<sub>2</sub> nanoparticles could not be detected due to the high LOD<sub>size</sub> (142–151 nm).

The variation in the concentration and (nano)particle percentage of TiO<sub>2</sub> and SiO<sub>2</sub> material throughout the *in vitro* gastrointestinal digestion process is presented in Table 4. Significant differences ( $p < 0.05$ ) in particle concentration were observed in all confectionery products for both particles when comparing their concentrations before and after the gastrointestinal digestion process with the major influence during the salivary step according to two-way ANOVA analysis.

The interactions of (nano)particles with proteins, carbohydrates, and salts throughout the gastrointestinal tract significantly influence their stability, aggregation state and biological effects (DeLoid et al., 2017; McClements et al., 2017). The proteins present in the salivary, gastric, and intestinal fluids, can lead to adsorption onto the (nano)particle surface and the formation of proteins corona, playing a key role in modulating the ability of (nano)particles to cross lipid bilayers and interact with intestinal epithelial cells (Treuel et al., 2014). For TiO<sub>2</sub> nanoparticles, Ranjan et al.(2018) demonstrated, using *in silico* methods, their strong affinity for binding to proteins in the cellular environment, particularly to charged amino acid residues (Liu, Meng, Pérez-Aguilar, &

Zhou, 2016). Similarly, carbohydrates can be adsorbed onto the surface of (nano)particles, forming a glycoconna (Sousa et al., 2021). These interactions could explain the results obtained in the current study. As shown in Table 3, no nanoparticulate material was detected in any of the bioaccessible extracts for TiO<sub>2</sub> (nano)particles. This could suggest the adsorption of TiO<sub>2</sub> nanoparticles may on proteins and/or carbohydrates from the gastrointestinal environment, leading to the formation of proteins corona and/or glycoconnas. However, this behavior was not observed for SiO<sub>2</sub> particles, likely due to differences in the intrinsic properties of the two types of (nano)particles.

As shown in Table 4, the particle percentage obtained with respect to the total amount of titanium and silicon is very low, suggesting most of titanium and silicon is present as ionic form in the extracts or as particles with a size below the LOD<sub>size</sub> of TiO<sub>2</sub> (30–64 nm) and LOD<sub>size</sub> of SiO<sub>2</sub> (142–151 nm). The percentage of particulate matter within this bio-accessible percentage in the intestinal stage was subsequently calculated as recommended by EFSA Scientific Committee (2018). Results in Table 4 reflected that the percentage of particles within the bio-accessible intestinal fraction for all confectionery products did not exceed 5 % for either titanium or silicon.

#### 3.4. Impact of *in vitro* digestion intestinal extracts from confectionaries on Caco-2 epithelial cells. Effect of SiO<sub>2</sub> and TiO<sub>2</sub> (nano) particles

The results obtained in the previous studies showed the presence of a low percentage of titanium and silicon (nano)particles available for their potential absorption in the intestinal epithelium. To evaluate the extent of this absorption, the Caco-2 cell line (epithelial cells isolated from colon tissues derived from human colorectal adenocarcinoma) commonly used for performing permeability studies was selected. For this purpose, an MTT assay exposing Caco-2 cells to the *in vitro* digestion

**Table 4**

Concentration of TiO<sub>2</sub> and SiO<sub>2</sub> (nano)particles and particle percentages before and across the gastrointestinal digestion process.

	<i>In vitro</i> stage	[TiO <sub>2</sub> ] <sub>0</sub> ·(10 <sup>6</sup> ) (Particle g <sup>-1</sup> )	TiO <sub>2</sub> particles (%)	[SiO <sub>2</sub> ] <sub>0</sub> ·(10 <sup>7</sup> ) (Particle g <sup>-1</sup> )	SiO <sub>2</sub> particles (%)
Pure cocoa	Water	260 ± 20*	18 ± 4*	82 ± 5*	4 ± 1
	Salivary	14 ± 1	4.3 ± 0.2	13 ± 1	6.5 ± 0.8
	Gastric	14 ± 2	3.0 ± 0.1	14 ± 2	7 ± 1
	Intestinal	15 ± 1	4.5 ± 0.2	12 ± 1	4 ± 1
Custard powder	Water	503 ± 35*	17 ± 5*	59 ± 4*	5 ± 1
	Salivary	13 ± 3	3.9 ± 0.2*	4 ± 1	6.4 ± 0.4
	Gastric	5 ± 1	1.3 ± 0.4	0.35 ± 0.04*	3 ± 1
	Intestinal	2 ± 1	1.5 ± 0.3	3 ± 1	6 ± 2
Soluble cocoa	Water	170 ± 10*	21 ± 4*	11 ± 1*	1.1 ± 0.2
	Salivary	50 ± 30*	7 ± 3*	6 ± 1	1.0 ± 0.2
	Gastric	7 ± 1	1.3 ± 0.2	9 ± 1	1.1 ± 0.2
	Intestinal	7 ± 1	3.1 ± 0.5	4 ± 1	2 ± 1

\* Indicates statistically significant differences ( $p < 0.05$ ) within the same column before (water) and under *in vitro* conditions (salivary, gastric and intestinal).

intestinal extracts of confectionary products was carried out.

Due to the complexity of the gastrointestinal extracts in terms of the food matrix components and enzymes used in the different steps of the process, it would not be correct to attribute the potential cell viability decrease to the merely presence of  $\text{TiO}_2$  and/or  $\text{SiO}_2$  (nano)particles. To understand the effect of Ti and Si in their different chemical forms (ionic and particulate  $\text{TiO}_2/\text{SiO}_2$ ) before exposing cells to gastrointestinal extracts, an MTT assay was conducted using ionic standards of titanium and silicon, anatase  $\text{TiO}_2$  nanoparticles, and  $\text{SiO}_2$  (nano)particles. The concentration ranges for each were chosen based on the concentrations found in intestinal fractions: ionic titanium ranging from  $20\text{--}40\ \mu\text{g L}^{-1}$ , ionic silicon from  $200\text{--}1000\ \mu\text{g L}^{-1}$ , anatase  $\text{TiO}_2$  nanoparticles from  $1\text{--}10\ \mu\text{g L}^{-1}$  ( $10^6\text{--}10^7\ \text{part g}^{-1}$ ), and  $\text{SiO}_2$  nanoparticles from  $1\text{--}10\ \mu\text{g L}^{-1}$  ( $10^6\text{--}10^7\ \text{part g}^{-1}$ ). Due to the simultaneous presence of the ionic and particulate forms of titanium and silicon, as well as of both elements in the confectionary products, the combined effect of the different chemical forms of both elements was evaluated within the low and high ranges of each selected concentration.

According to Fig. 2 a), b), and c), no significant differences were found in the cell viability of Caco-2 cells after exposure during 4 and 24 h to the different chemical forms of titanium and silicon either together or individually.

Considering that enzymes present in intestinal extracts could

contribute to the absorbance in the MTT assay, several dilution factors of 1/5, 1/10, and 1/25 of the intestinal blanks (*in vitro* digestion intestinal extracts without containing confectionary products) were applied to the cells at 4 and 24 h of exposure. The optimal dilution selected was 1/10, as it did not affect cell viability after exposure to cells for 4 and 24 h. When cells were exposed to the intestinal extracts, resulting from the *in vitro* gastrointestinal digestion process of the confectionary products, cell viability decreased more pronounced at 24 h as compared to 4 h. Comparing cell viability at both exposure times, in pure cocoa, percentages of cell viability of  $83 \pm 4\%$  and  $25 \pm 5\%$  in pure cocoa,  $71 \pm 6\%$  and  $41 \pm 1\%$ , in custard and  $75 \pm 2\%$  and  $44 \pm 2\%$  in soluble cocoa, for 4 h and 24 h of exposure, respectively were obtained all values referenced to the positive control, which exhibited  $96 \pm 4\%$  viability.

Several studies in the literature have been reported about the cytotoxicity of  $\text{SiO}_2$  and  $\text{TiO}_2$  (nano)particles by using different cell lines. However, no data was found in the literature regarding the exposure of Caco-2 cells to *in vitro* digestion intestinal extracts from real samples. Based on the results obtained from exposure to the standards (Fig. 2 a), b), and c)), the decrease in cell viability following exposure to intestinal food extracts (Fig. 2 d)) cannot be attributed neither to the presence of  $\text{TiO}_2$  and/or  $\text{SiO}_2$  particles, nor to their ionic forms (titanium and/or silicon). Therefore, this cytotoxic effect may be triggered by other endogenous components present in the matrix of confectionery

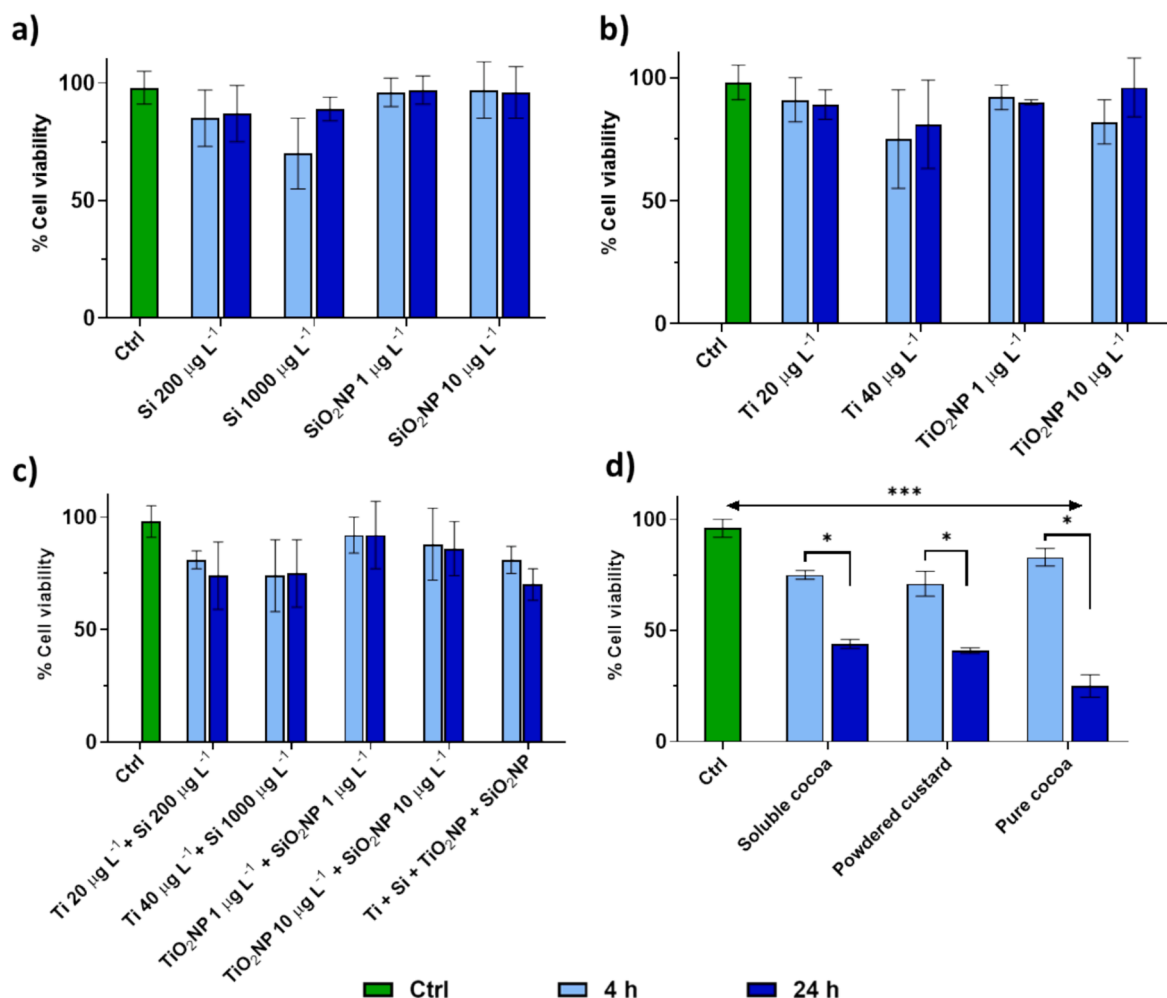


Fig. 2. Caco-2 cell viability percentage once exposed to a) ionic (titanium) and particulate ( $\text{TiO}_2$ ) titanium, b) ionic (silicon) and particulate ( $\text{SiO}_2$ ) silicon, c) both titanium and silicon in ionic and particulate forms, and d) soluble cocoa, custard powder and pure cocoa *in vitro* digestion intestinal extracts (diluted 1/10). Data obtained via MTT assay.

\* Indicates statistically significant differences ( $p < 0.05$ ) between 4 and 24 h of exposition time.

\*\*\* Indicates statistically significant differences ( $p < 0.05$ ) between cells controls and intestinal food extracts from *in vitro* digestion.

products. In the present study, although particles of SiO<sub>2</sub> smaller than 151 nm were not detected and quantified in the intestinal extracts (LOD size by spICP-MS for intestinal stage), they could influence the cell viability. However, results in Table 4 suggest the aggregation/agglomeration of these particles during *in vitro* assay, especially during the salivary step.

Hsiao et al.(2014) conducted MTT assays to investigate how SiO<sub>2</sub> particle size and its concentration affected various macrophages and cell lines, including A549 (Adenocarcinoma human alveolar basal epithelial cells). They investigated exposure durations of 24 h to SiO<sub>2</sub> particles with sizes of 5, 60, and 200 nm, covering concentrations from 0 to 50 µg mL<sup>-1</sup>. Results revealed that smaller particles exhibited higher cytotoxicity in A549 cells, and this effect was dependent on the concentration. However, for 200 nm particles, there was no significant reduction in cell viability, regardless of exposure concentration as observed in the current study with SiO<sub>2</sub> particles of the same size (Fig. 2a). Similar outcomes were observed by Lu et al.(2011) and Mu et al.(2012) when studying the cytotoxicity of 7–50 nm SiO<sub>2</sub> nanoparticles on HepG2 (Human hepatoma) and HT29 (human colorectal adenocarcinoma) cells respectively, revealing that cell viability is influenced by both dose and particle size at 24 h of exposure. However, results reported by Docter et al.(2014) highlighted a significant decrease in cell viability, due to the loss of membrane integrity, when exposing increasing concentrations of 30 nm SiO<sub>2</sub> nanoparticles for 4 and 24 h on the Caco-2 cell line.

The results of the present study cannot be directly compared to those obtained by Ferrante et al.(2023), who exposed increasing concentrations of TiO<sub>2</sub> derived from the food additive E171 to the colon cancer cell lines Caco-2 and HCT-116 for 72 h. Also, the studies conducted by Sun et al.(2017), revealed the influence of both size and morphology of TiO<sub>2</sub> particles of 100, 200, and 300 nm on the toxicity in the NCI-H292 Mucoepidermoid Pulmonary carcinoma cell line. The results highlighted a decrease in cell viability with increasing particle size. Additionally, the mechanism of cell death also varied depending on the particle size. It should be noted that the aforementioned studies have not been conducted with standard suspensions of particulate material alone without considering the effect of food matrix, where (nano)particles are presented.

#### 4. Conclusions

The evaluation of the risk associated with nanoparticle forms in food additives, such as TiO<sub>2</sub> (E171, banned in Europe) and SiO<sub>2</sub> (E551), requires in-depth knowledge of their physicochemical properties before and after oral ingestion and their potential to induce cytotoxic effects. Results from the application of an *in vitro* gastrointestinal assay from the selected confectionary products revealed no significant changes in size distribution throughout the *in vitro* gastrointestinal process. TiO<sub>2</sub> nanoparticles were detected at concentrations below 50 % of total Ti concentration. The percentages of bioaccessibility found for TiO<sub>2</sub> and SiO<sub>2</sub> were very low not exceeding 5 % and 6 %, respectively. The cytotoxicity results showed a decrease in Caco-2 cell viability after 24 h of exposure to intestinal extracts from confectionery products, indicating a cytotoxic effect. However, this effect was not due to the presence of (nano)particles themselves but to the components of food matrix. While the bioaccessible concentrations of particles alone did not significantly affect cell viability, the full gastrointestinal extracts caused a substantial decrease, likely due to other food constituents.

These findings highlight the importance of including food matrices in cytotoxicity studies, as the mere use of pristine (nano)particles standard solutions may overestimate their effects and underestimate the influence of food components. This approach provides a more realistic assessment of their impact on real-world dietary scenarios. This study is the first reported in the literature that considers the combined impact of TiO<sub>2</sub> and SiO<sub>2</sub> (nano)particles and food matrix.

#### CRedit authorship contribution statement

**Elena Espada-Bernabé:** Writing – review & editing, Writing – original draft, Validation, Methodology, Investigation, Conceptualization. **Gustavo Moreno-Martín:** Writing – review & editing, Writing – original draft, Validation, Methodology, Investigation. **Beatriz Gómez-Gómez:** Writing – review & editing, Writing – original draft, Validation, Methodology, Investigation, Conceptualization. **Yolanda Madrid:** Writing – review & editing, Writing – original draft, Validation, Resources, Methodology, Funding acquisition.

#### Declaration of competing interest

The authors declare that they have no known competing financial interests or personal relationships that could have appeared to influence the work reported in this paper.

#### Acknowledgements

The authors thank the Spanish Commission of Science and Technology (PID2020-114714RB-I00 and PID2023-148425NB-I00) and the Community of Madrid through a research support contract (CT4/21-CT5/21).

#### Appendix A. Supplementary data

Supplementary data to this article can be found online at <https://doi.org/10.1016/j.foodres.2025.115754>.

#### Data availability

Data will be made available on request.

#### References

- Baranowska-Wójcik, E., Szwajgier, D., & Winiarska-Mieczan, A. (2022). A review of research on the impact of E171/TiO<sub>2</sub> NPs on the digestive tract. *Journal of Trace Elements in Medicine and Biology*, 72(126988). <https://doi.org/10.1016/j.jtemb.2022.126988>
- Bastardo-Fernández, I., Chekri, R., Noireaux, J., Fiscaro, P., & Jitaru, P. (2023). Characterisation and quantification of titanium dioxide nanoparticles in food simulants by single particle inductively coupled plasma-tandem mass spectrometry using a high efficiency sample introduction system. *Spectrochimica Acta - Part B. Atomic Spectroscopy*, 208(September). <https://doi.org/10.1016/j.sab.2023.106782>
- Bettencourt, A., Gonçalves, L. M., Gramacho, A. C., Vieira, A., Rolo, D., Martins, C., & Louro, H. (2020). Analysis of the characteristics and cytotoxicity of titanium dioxide nanomaterials following simulated *in vitro* digestion. *Nanomaterials*, 10(8), 1–18. <https://doi.org/10.3390/nano10081516>
- Bolea-Fernández, E., Leite, D., Rua-Ibarz, A., Balcaen, L., Aramendia, M., Resano, M., & Vanhaecke, F. (2017). Characterization of SiO<sub>2</sub> nanoparticles by Single Particle-Inductively Coupled Plasma-Tandem Mass Spectrometry (SP-ICP-MS/MS). *Journal of Analytical Atomic Spectrometry*, 1–43. <https://doi.org/10.1039/C7JA00138J>
- Brar, S. K., & Verma, M. (2011). Measurement of nanoparticles by light-scattering techniques. *TrAC - Trends in Analytical Chemistry*, 30(1), 4–17. <https://doi.org/10.1016/j.trac.2010.08.008>
- Bucher, G., & Auger, F. (2019). Combination of <sup>47</sup>Ti and <sup>48</sup>Ti for the determination of highly polydisperse TiO<sub>2</sub> particle size distributions by spICP-MS. *Journal of Analytical Atomic Spectrometry*, 34(7), 1380–1386. <https://doi.org/10.1039/c9ja00101h>
- Cao, X., Zhang, T., DeLoid, G. M., Gaffrey, M. J., Weitz, K. K., Thrall, B. D., ... Demokritou, P. (2020). Evaluation of the cytotoxic and cellular proteome impacts of food-grade TiO<sub>2</sub> (E171) using simulated gastrointestinal digestions and a tri-culture small intestinal epithelial model. *NanoImpact*, 17. <https://doi.org/10.1016/j.impact.2019.100202>
- Chen, H., Zhao, R., Wang, B., Cai, C., Zheng, L., Wang, H., ... Feng, W. (2017). The effects of orally administered Ag, TiO<sub>2</sub> and SiO<sub>2</sub> nanoparticles on gut microbiota composition and colitis induction in mice. *NanoImpact*, 8(March), 80–88. <https://doi.org/10.1016/j.impact.2017.07.005>
- DeLoid, G. M., Wang, Y., Kapronezai, K., Lorente, L. R., Zhang, R., Pyrgiotakis, G., Konduru, N. V., Ericsson, M., White, J. C., De La Torre-Roche, R., Xiao, H., McClements, D. J., & Demokritou, P. (2017). An integrated methodology for assessing the impact of food matrix and gastrointestinal effects on the biokinetics and cellular toxicity of ingested engineered nanomaterials. *Particle and Fibre Toxicology*, 14(1). <https://doi.org/10.1186/s12989-017-0221-5>
- Docter, D., Bantz, C., Westmeier, D., Galla, H. J., Wang, Q., Kirkpatrick, J. C., Nielsen, P., Maskos, M., & Stauber, R. H. (2014). The protein corona protects against size- and

- dose-dependent toxicity of amorphous silica nanoparticles. *Beilstein Journal of Nanotechnology*, 5(1), 1380–1392. <https://doi.org/10.3762/bjnano.5.151>
- EFSA, P. on F. A. and N. S. added to F. (2018). Re-evaluation of silicon dioxide (E 551) as a food additive. *EFSA Journal*, 16(1), 1–70. doi: 10.2903/j.efsa.2018.5088.
- EFSA Panel on Food Additives and Flavourings (FAF). (2019). Scientific opinion on the proposed amendment of the EU specifications for titanium dioxide (E 171) with respect to the inclusion of additional parameters related to its particle size distribution. *EFSA Journal*, 17(7). <https://doi.org/10.2903/j.efsa.2019.5760>
- EFSA Scientific Committee. (2018). Guidance on risk assessment of the application of nanoscience and nanotechnologies in the food and feed chain: Part 1, human and animal health. *EFSA Journal*, 16(7). <https://doi.org/10.2903/j.efsa.2018.5327>
- Espada-Bernabé, E., Moreno-Martín, G., Gómez-Gómez, B., & Madrid, Y. (2024). Assessing the behaviour of particulate/nanoparticulate form of E171 (TiO<sub>2</sub>) food additive in colored chocolate candies before and after in vitro oral ingestion by spICP-MS, TEM and cellular in vitro models. *Food Chemistry*, 432(May 2023). <https://doi.org/10.1016/j.foodchem.2023.137201>
- Ferrante, M., Grasso, A., Salemi, R., Libra, M., Tomasello, B., Fiore, M., & Copat, C. (2023). DNA Damage and Apoptosis as In-Vitro Effect Biomarkers of Titanium Dioxide Nanoparticles (TiO<sub>2</sub>-NPs) and the Food Additive E171 Toxicity in Colon Cancer Cells: HCT-116 and Caco-2. *International Journal of Environmental Research and Public Health*, 20(3). <https://doi.org/10.3390/ijerph20032002>
- Ferraris, F., Raggi, A., Ponti, J., Mehn, D., Gilliland, D., Savini, S., Iacononi, F., Aureli, F., Calzolari, L., & Cubadda, F. (2023). Agglomeration Behavior and Fate of Food-Grade Titanium Dioxide in Human Gastrointestinal Digestion and in the Lysosomal Environment. *Nanomaterials*, 13(13). <https://doi.org/10.3390/nano13131908>
- Geiss, O., Ponti, J., Senaldi, C., Bianchi, L., Mehn, D., Barrero, J., Gilliland, D., Matissek, R., & Anklam, E. (2020). Characterisation of food grade titania with respect to nanoparticle content in pristine additives and in their related food products. *Food Additives and Contaminants - Part A Chemistry, Analysis, Control, Exposure and Risk Assessment*, 37(2), 239–253. <https://doi.org/10.1080/19440049.2019.1695067>
- Givelet, L., Truffier-Boutry, D., Noël, L., Damlencourt, J. F., Jitaru, P., & Guérin, T. (2021). Optimisation and application of an analytical approach for the characterisation of TiO<sub>2</sub> nanoparticles in food additives and pharmaceuticals by single particle inductively coupled plasma-mass spectrometry. *Talanta*, 224. <https://doi.org/10.1016/j.talanta.2020.121873>
- Guilloteau, E., Djouina, M., Caboche, S., Waxin, C., Deboudt, K., Beury, D., Hot, D., Pichavant, M., Dubuquoy, L., Launay, D., Vignal, C., Choël, M., & Body-Malapel, M. (2022). Exposure to atmospheric Ag, TiO<sub>2</sub>, Ti and SiO<sub>2</sub> engineered nanoparticles modulates gut inflammatory response and microbiota in mice. *Ecotoxicology and Environmental Safety*, 236(November 2021). doi: 10.1016/j.ecoenv.2022.113442.
- Hsia, I. L., Mareike Gramatke, A., Joksimovic, R., Sokolowski, M., Grdzielski, M., & Haase, A. (2014). Size and Cell Type Dependent Uptake of Silica Nanoparticles. *Journal of Nanomedicine & Nanotechnology*, 05(06). <https://doi.org/10.4172/2157-7439.1000248>
- IUPAC, I. U. of P. and A. C. (1978). Nomenclature, symbols, units and their usage in spectrochemical analysis—III. Analytical Flame Spectroscopy and Associated Non-flame Procedures. *Spectrochimica Acta Part B: Atomic Spectroscopy*, 33(6), 247–269. doi: 10.1016/0584-8547(78)80045-7.
- Jovanović, B. (2014). Critical review of public health regulations of titanium dioxide, a human food additive. *Integrated Environmental Assessment and Management*, 11(1), 10–20. <https://doi.org/10.1002/ieam.1571>
- Kesteren, P. C. E. Van, Cubadda, F., Bouwmeester, H., Eijkeren, J. C. H. Van, & Dekkers, S. (2014). Novel insights into the risk assessment of the nanomaterial synthetic amorphous silica, additive E551, in food. August. doi: 10.3109/17435390.2014.940408.
- Laborda, F., Bolea, E., Cepriá, G., Gómez, M. T., Jiménez, M. S., Pérez-Arategui, J., & Castillo, J. R. (2016). Detection, characterization and quantification of inorganic engineered nanomaterials: A review of techniques and methodological approaches for the analysis of complex samples. *Analytica Chimica Acta*, 904, 10–32. <https://doi.org/10.1016/j.aca.2015.11.008>
- Laborda, F., Bolea, E., & Jiménez-Lamana, J. (2014). Single Particle Inductively Coupled Plasma Mass Spectrometry: A Powerful Tool for Nanoanalysis. *Analytical Chemistry*, 86(5), 2270–2278. <https://doi.org/10.1021/ac402980q>
- Laborda, F., Giménez-Ingalaturre, A. C., Bolea, E., & Castillo, J. R. (2020). About detectability and limits of detection in single particle inductively coupled plasma mass spectrometry. *Spectrochimica Acta - Part B Atomic Spectroscopy*, 169(May), Article 105883. <https://doi.org/10.1016/j.sab.2020.105883>
- Liu, S., Meng, X. Y., Pérez-Aguilar, J. M., & Zhou, R. (2016). An in Silico study of TiO<sub>2</sub> nanoparticles interaction with twenty standard amino acids in aqueous solution. *Scientific Reports*, 6(October), 1–10. <https://doi.org/10.1038/srep37761>
- Lu, X., Qian, J., Zhou, H., Gan, Q., Tang, W., Lu, J., Yuan, Y., & Liu, C. (2011). In vitro cytotoxicity and induction of apoptosis by silica nanoparticles in human HepG2 hepatoma cells. *International Journal of Nanomedicine*, 6, 1889–1901.
- McClements, D. J., DeLoId, G., Pyrgiotakis, G., Shatkin, J. A., Xiao, H., & Demokritou, P. (2016). The role of the food matrix and gastrointestinal tract in the assessment of biological properties of ingested engineered nanomaterials (iENMs): State of the science and knowledge gaps. In *NanoImpact* (Vols. 3–4, pp. 47–57). Elsevier B.V. doi: 10.1016/j.impact.2016.10.002.
- McClements, D. J., Xiao, H., & Demokritou, P. (2017). Physicochemical and colloidal aspects of food matrix effects on gastrointestinal fate of ingested inorganic nanoparticles. *Advances in Colloid and Interface Science*, 246, 165–180. <https://doi.org/10.1016/j.cis.2017.05.010>
- Mech, A., Rauscher, H., Babick, F., Hodoroaba, V.-D., Ghanem, A., Wohlleben, W., Marvin, H., Weigel, S., Brünel, R., & Friedrich, C. M. (2020). The NanoDefine Methods Manual Part 3: Standard operating Procedures (SOPs). In *Publications Office of the European Union, Luxembourg* (p. 215). JCR117501. doi: 10.2760/778.
- Mozhayeva, D., & Engelhard, C. (2020). A critical review of single particle inductively coupled plasma mass spectrometry—A step towards an ideal method for nanomaterial characterization. *Journal of Analytical Atomic Spectrometry*, 35(9), 1740–1783. <https://doi.org/10.1039/c9ja00206e>
- Mu, Q., Hondow, N. S., Krzemi, Ł., Brown, A. P., Jeuken, L. J. C., & Routledge, M. N. (2012). Mechanism of cellular uptake of genotoxic silica nanoparticles. *Particle and Fibre Toxicology*, 9(29), 1–11. <https://doi.org/10.1186/1743-8977-9-29>
- Musial, J., Krakowiak, R., Mlynarczyk, D. T., Goslinski, T., & Stanisz, B. J. (2020). Titanium dioxide nanoparticles in food and personal care products—What do we know about their safety? In *Nanomaterials* (Vol. 10, Issue 6, pp. 1–23). MDPI AG. doi: 10.3390/nano10061110.
- Pace, H. E., Rogers, N. J., Jarolimek, C., Coleman, V. A., Higgins, C. P., & Ranville, J. F. (2011). Determining transport efficiency for the purpose of counting and sizing nanoparticles via single particle inductively coupled plasma mass spectrometry. *Analytical Chemistry*, 83, 9361–9369. <https://doi.org/10.1021/ac300942m>
- Peters, R., Herrera-Rivera, Z., Undas, A., Van Der Lee, M., Marvin, H., Bouwmeester, H., & Weigel, S. (2015). Single particle ICP-MS combined with a data evaluation tool as a routine technique for the analysis of nanoparticles in complex matrices. *Journal of Analytical Atomic Spectrometry*, 30(6), 1274–1285. <https://doi.org/10.1039/c4ja00357h>
- Peters, R. J. B., Bommel, G. V., Herrera-Rivera, Z., Helsen, H. P. F. G., Marvin, H. J. P., Weigel, S., ... Bouwmeester, H. (2014). Characterization of Titanium Dioxide Nanoparticles in Food Products: Analytical Methods To Define Nanoparticles. *Journal of Agricultural and Food Chemistry*, 62, 6285–6293. <https://doi.org/10.1021/jf5011885>
- Peters, R., Kramer, E., Oomen, A. G., Rivera, Z. E. H., Oegema, G., Tromp, P. C., ... Bouwmeester, H. (2012). Presence of Nano-Sized Silica during In Vitro Digestion of Foods Containing Silica as a Food Additive. *ACS Nano*, 6(3), 2441–2451. <https://doi.org/10.1021/nm204728k>
- Ranjana, S., Dasgupta, N., Sudandiradoss, C., Ramalingam, C., & Kumar, A. (2018). Titanium dioxide nanoparticle–protein interaction explained by docking approach. *International Journal of Nanomedicine*, 13, 47–50. <https://doi.org/10.2147/IJN.S125008>
- Sousa, A. A., Schuck, P., & Hassan, S. A. (2021). Biomolecular interactions of ultrasmall metallic nanoparticles and nanoclusters. *Nanoscale Advances*, 3(11), 2995–3027. <https://doi.org/10.1039/d1na00086a>
- Sun, Q., Ishii, T., Kanehira, K., Sato, T., & Taniguchi, A. (2017). Uniform TiO<sub>2</sub> nanoparticles induce apoptosis in epithelial cell lines in a size-dependent manner. *Biomaterials Science*, 5(5), 1014–1021. <https://doi.org/10.1039/c6bm00946h>
- Tada-Oikawa, S., Ichihara, G., Fukatsu, H., Shimanuki, Y., & Tanaka, N. (2016). Titanium Dioxide Particle Type and Concentration Influence the Inflammatory Response in Caco-2 Cells. *International Journal of Molecular Sciences*, 576(17). <https://doi.org/10.3390/ijms17040576>
- Talamini, L., Gimondi, S., Violatto, M. B., Fiordaliso, F., Tran, N. L., Sitia, G., Aureli, F., Raggi, A., Cubadda, F., Bigini, P., Diomedea, L., Talamini, L., Gimondi, S., Violatto, M. B., Fiordaliso, F., Tran, N. L., Sitia, G., Aureli, F., Raggi, A., & Nelissen, I. (2019). Repeated administration of the food additive E171 to mice results in accumulation in intestine and liver and promotes an inflammatory status. *Nanotoxicology*, 1–15. <https://doi.org/10.1080/17435390.2019.1640910>
- The European Commission. (2022). COMMISSION REGULATION (EU) 2022/63 of 14 January 2022 amending Annexes II and III to Regulation (EC) No 1333/2008 of the European Parliament and of the Council as regards the food additive titanium dioxide (E 171). *Official Journal of the European Union*.
- Treuel, L., Brandholt, S., Maffre, P., Wiegele, S., Shang, L., & Nienhaus, G. U. (2014). Impact of protein modification on the protein corona on nanoparticles and nanoparticle-cell interactions. *ACS Nano*, 8(1), 503–513. <https://doi.org/10.1021/nn405019v>
- Verleysen, E., Wagner, T., Lipinski, H. G., Kägi, R., Koeber, R., Boix-Sanfelieu, A., De Temmerman, P. J., & Mast, J. (2019). Evaluation of a TEM based approach for size measurement of particulate (nano)materials. *Materials*, 12(14). <https://doi.org/10.3390/ma12142274>
- Yan, J., Chen, Q., Tian, L., Li, K., Lai, W., Bian, L., Han, J., Jia, R., Liu, X., & Xi, Z. (2022). Intestinal toxicity of micro- and nano-particles of foodborne titanium dioxide in juvenile mice: Disorders of gut microbiota–host co-metabolites and intestinal barrier damage. *Science of the Total Environment*, 821, Article 153279. <https://doi.org/10.1016/j.scitotenv.2022.153279>